Preferred citation: F. Golkhosh, Y. Sharma, D.M. Martinez, W. Tsai, L. Courtois, D. Eastwood, P.D. Lee and A.B. Phillion. Synchroton tomographic imaging of softwood paper: A 4D investigation of deformation and failure mechanism. In **Advances in Pulp and Paper Research, Oxford 2017**, *Trans. of the XVIth Fund. Res. Symp. Oxford, 2017*, (W. Batchelor and D. Söderberg, eds), pp 611–625, FRC, Manchester, 2018. DOI: 10.15376/frc.2017.2.611.

SYNCHROTRON TOMOGRAPHIC IMAGING OF SOFTWOOD PAPER: A 4D INVESTIGATION OF DEFORMATION AND FAILURE MECHANISM

F. Golkhosh[1], Y. Sharma[2], D. M. Martinez[3], W. Tsai[3, 4], L. Courtois[5], D. Eastwood[5], P. D. Lee[5] and A. B. Phillion[6]

[1] School of Engineering, The University of British Columbia, Canada
[2] Chair of Biomedical Physics, Department of Physics and School of BioEngineering, Technical University of Munich, Germany
[3] Dept. of Chemical and Biological Engineering, The University of British Columbia, Canada
[4] Canfor Pulp Innovation, Canfor Pulp, Canada
[5] Manchester X-ray Imaging Facility, University of Manchester, UK
[6] Dept of Materials Science and Engineering, McMaster University, Canada

ABSTRACT

Fibre pull-out and fibre fracture are the two dominant failure mechanisms of softwood paper. For the first time, 4D synchrotron X-ray tomographic imaging (three spatial directions plus time) was performed to observe these mechanisms in-situ during tensile deformation of softwood paper handsheets. The experiments were conducted on three handsheets, produced from pulp that was low consistency refined at 0 k Wh/t and 100 kWh/t and either air-dried in restraint or freeze-dried. The fibre deformation was found to be highly complex; initially being accommodated via straightening of the fibres resulting in fibre

separation and then complete fibre pull-out or fibre fracture. The 3D strain fields, computed by Digital Volume Correlation, revealed increasing out-of-plane deformation in samples with decreasing inter-fibre bonding. Further, the relation between the L2 norms of the out-of-plane strain fields with displacement was computed and found to follow a second order polynomial, with an increasing slope in samples with reduced inter-fibre bonding. It was then shown that the accumulated out-of-plane deformations could be used as a metric to quantify the relative contribution of inter-fibre bond breakage, and subsequently, fibre pull-out during tensile deformation of handsheets. The results demonstrate that 4D imaging provides new insights into paper deformation mechanisms

1 INTRODUCTION

Inter-fibre bond breakage and fibre fracture are the main mechanisms responsible for plastic deformation and failure of paper sheets. The relative importance of these mechanisms has long been the subject of research within the paper community. Some researchers have postulated that disruption of inter-fibre bonds occurs during all stages of deformation, along with elastic strain of the fibres [1], [2]. However, others have theorized that plasticity within paper is a result of irreversible deformation of the fibre's cell walls [3], [4]. Further, paper is known to be an auxetic material, exhibiting thickness expansion during in-plane tensile deformations [5], [6], [7], [8]. This uncommon material property is believed to originate from the straightening of fibres [6], [8], which causes them to separate. It is thought that hydrogen bonding also plays a significant role in controlling the degree of auxetic behaviour [8].

It is well known that the paper making processes will strongly influence the extent of inter-fibre bonding by altering both the Campbell effect during drying [9], [10] and the conformability of fibres during the refining process [11]. In this study, a new methodology known as 4D (three spatial dimensions plus time) imaging via synchrotron X-ray computed tomography (sCT) is applied to investigate the linkages between paper making process parameters and tensile deformation of softwood paper handsheets. The acquired high-resolution 3D datasets, captured at different stages of deformation, are used to quantify the evolution of the fibre network. This allows for characterization of the underlying mechanisms linking refining, deformation, and failure of a paper sheet. In addition, the use of non-contact imaging allows for direct measurement of the out-of-plane deformations without mechanical contacts that are prone to significant experimental error and are limited in scope.

2 METHODS

4D imaging to investigate the effects of processing on deformation mechanisms was performed by combining purpose-created handsheets, synchrotron X-ray tomographic imaging (sCT), and a bespoke tensile tester suitable for sCT.

2.1 Sample preparation

Three standard handsheets, referred to as freeze-dried, non-refined, and highly-refined, were created for this study using the facilities at The University of British Columbia (UBC)'s Pulp and Paper Centre. The base material was an NBSK pulp provided by Canfor. The three samples were made of: un-refined and freeze-dried pulp, un-refined and air-dried pulp, and Low-Consistency (LC) refined and air-dried pulp. The LC refining was performed at a specific refining energy of 100 kWh/t. The air drying was carried out, after formation of the sheets, in restraint at 23 °C and 50% RH for 24 hours. The handsheets, having an areal density of 60 g/m^2, were formed using a British handsheet maker and following standard TAPPI procedures.

2.2 Tensile test sample design and grip methodology

The handsheets were cut into samples having a dog-bone shape as depicted in Figure 1(a): 18 mm long with a gauge length (width) of 2.8 (3.0) mm. The dog-bone shape was used to ensure that fracture would occur within the field of view during sCT imaging. The non- and highly-refined samples were cut using a Silver Bullet™ paper cutter at UBC. Due to their delicacy, the freeze-dried samples were cut using a laser cutter at University College London.

The test methodology was carefully designed to avoid damaging the tensile samples. Four identical samples, Figure 1(b) (3 for the freeze-dried condition), were deformed concurrently using 3D-printed tensile grips, Figure 1(c). This multi-sample test setup was required to increase the load to a measurable value of ~20 N. A pin-grip was used to link the paper samples to each other, as well as to the tensile tester. To ensure that fracture did not occur at the pin-holes during tensile deformation, a screw and nut setup was used to apply adjustable compressive loading. Small rectangular spacers were used to separate the samples so that they were easily distinguishable in the 3D images, and also to aid load transfer. An adhesive tape was applied between each sample and its adjacent spacers for reinforcement. Note that the U-shape bracket seen in the Figure 1(c) was used to facilitate sample handling without damaging the samples; this was taken out after the grips were placed in the tensile tester.

2.3 4D imaging of softwood deformation

The 4D imaging experiments were performed on the I13 beamline at the Diamond Light Source (Didcot, UK) under pink beam conditions using a bespoke tensile tester known as the P2R [12]. Figure 2 depicts the placement of the 3D printed grips in the P2R. The samples were deformed in tension in an incremental fashion

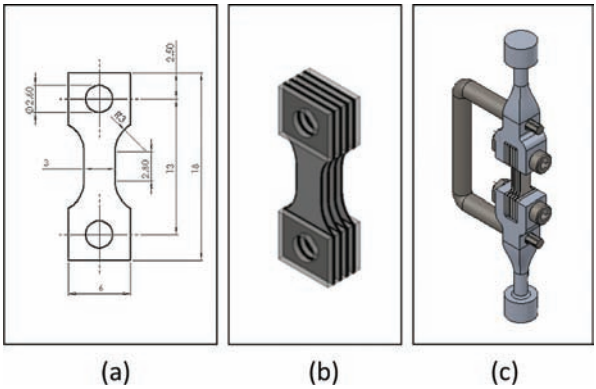

Figure 1. (a) Sample geometry and dimensions; (b) configuration of multiple samples and spacers; (c) overall assembly of sample with 3D printed grips for tensile testing using the P2R.

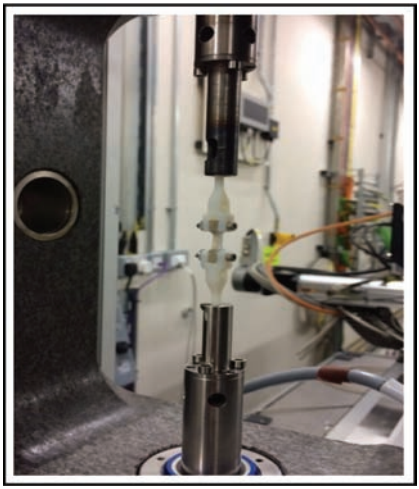

Figure 2. Image showing grip assembly mounted within the P2R tensile tester.

in steps of 100 μm, with deformation applied at a rate of 100 μm/min, followed by a 2-minute relaxation time and subsequent acquisition of the 3D image at a voxel size of 1.6 μm and a field of view of 64 mm^3. In total, each sample was deformed in ~18–20 steps prior to failure, with 3D images captured at each step. Note that some samples contained areas of yellow/brown discolouration after the 4D imaging, providing indication that the intensity of the X-ray beam damaged the handsheets.

2.4 Image analysis

After acquisition of the time-resolved sequence of 3D images, the Avizo Image Analysis software (Thermo Fisher Scientific, USA) was used to qualitatively observe the deformation process, and the VicVolume Digital Volume Correlation (DVC) software (Correlated Solutions, USA) was used to quantify the structural changes occurring within the paper samples. In contrast to 2D Digital Image Correlation, DVC [13] can also quantify out-of-plane deformations, which has been previously largely overlooked in paper physics research.

Figure 3 provides a schematic diagram of the DVC process. As shown in the top-left image, the reference model is divided into several identical cubic sub volumes or regions of interest. Each sub volume, labeled as k_0, is defined as a set

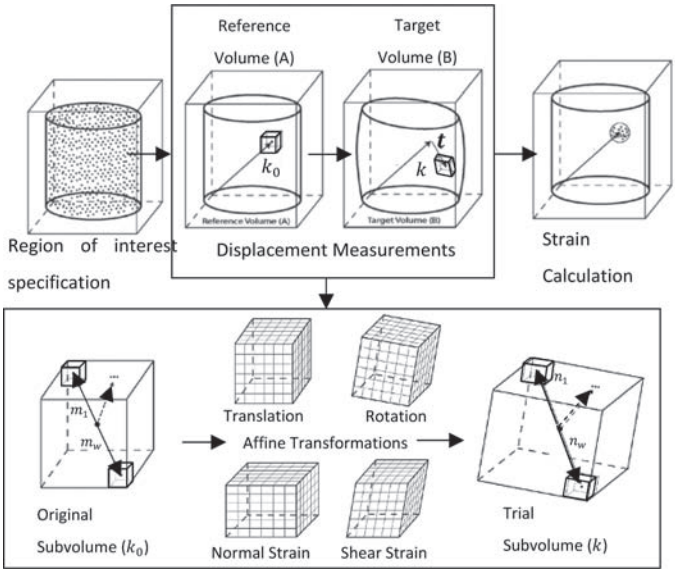

Figure 3. Schematic diagram of the DVC process [14].

of w vectors centred at the middle of the sub volume and pointing to individual sub elements, $\{\boldsymbol{m}^{\alpha}: \alpha = 1,2,3, \ldots, w\}$, as shown in the bottom-left image. The DVC algorithm computes the displacement vectors, labeled as $\boldsymbol{t}$ in the top middle part of the image, at each measurement point by correlating the reference sub volume with the target (deformed) sub volume. First, a series of trial sub volumes, labeled as k in the bottom-right image, are computed by applying a series of affine transformations (translation, rotation, normal strain, and shear strain) to the original sub volume k_0. Then, each trial sub volume is compared against values extracted from the target volume $\{\boldsymbol{n}^{\alpha}: \alpha = 1,2,3, \ldots, w\}$ using a correlation function to quantify the degree of match between the two states. Gradient-based methods are used to iteratively identify candidate trial sub volumes until the correlation coefficient is minimized. A threshold value is then used to exclude the values that are above a certain value to achieve a suitable confidence in the results. Finally, the corresponding strain tensors are computed using Lagrangian or Eulerian descriptors.

3 RESULTS AND DISCUSSIONS

3.1 Qualitative observations of deformation in the freeze-dried sample

Figure 4 shows the front-view (1) and side-view (2) of the freeze-dried sample in the (a) reference state and (b)–(d) after tensile deformations of 1200 μm, 1600 μm and 2580 μm, respectively. By comparing these images, the evolution of the fibre network resulting from tensile deformation can be observed. First, between Figures 4(a)-1 and 4(b)-1, it seems that the fibres have become more visible, especially in the bottom of the image. A closer look at the side-views of the sample at the same deformation states, Figures 4(a)-2 and 4(b)-2, reveals some out-of-plane expansion at the bottom of the sample. Second, the initial signs of failure are already evident in the lower region of Figure 4(c)-1, after deformation of 1600 μm has been applied. Specifically, there is a large area that seem to be less dense when compared to the reference state, indicating fibre pull-out. This is made further clear in Figure 4(d)-1, with 2580 μm of deformation, as there are a large number of fibres at the bottom of the sample that seem to be aligned in the direction of the load, further indicating fibre pull-out. Although no rupture zone (in its conventional form) was observed during the failure of this sample, failure was identified to occur at 1200 μm by a drop in the load measured by the tensile tester. The measured loads will be discussed in Section 3.3 Fibre pull-out in this sample was expected to occur, since the freeze-drying process results in extremely weak inter-fibre bonds due to a reduction in the Campbell effect [10]. The handsheet's weakness is magnified by the low conformability of the constituent fibres that have not been refined [11].

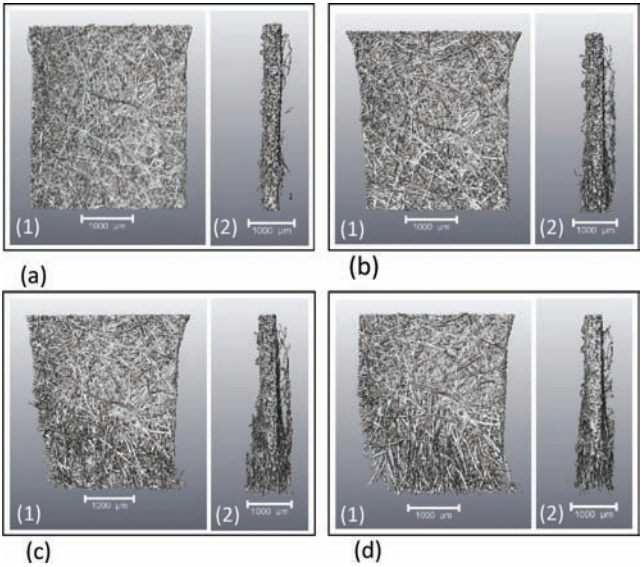

Figure 4. (1) Front-view and (2) side-view visualization of the freeze-dried sample in (a) reference state, (b) deformation of 1200 μm, (c) deformation of 1600 μm, and (d) deformation of 2580 μm.

A comparison between the side view images of Figure 4(a)/4(c), 4(b)/4(d) shows an increase in the sample thickness with increasing deformation. This thickness expansion was most pronounced at the bottom of the sample, inside the failure region. This observed thickness expansion is contrary to the hypothesis made in [8] that there will not be significant increase in sheet thickness during deformation of paper samples having weak hydrogen bonding, like freeze dried handsheets, since the fibres would simply slide past each other and have significant opportunity to occupy the empty spaces.

Figure 5(a) provides an overview of the fibre structure at a deformation of 1200 μm with four manually segmented fibres highlighted in a region of interest. Figure 5(b) shows three horizontal slices of the same cross-section in the (b)-1 reference state, (b)-2 1000μm, and (b)-3 1200 μm displacement states. A comparison between Figures 5(b)-1 and 5(b)-2 reveals that after 1000 μm of displacement, only the red fibre has sustained any deformation; the remaining fibres do not appear deformed nor displaced. By 1200 μm of displacement, the blue fibre has clearly detached from the red fibre, and also appears to have deformed.

Although Figure 5(b) provides some ability to study fibre deformation, it is quite difficult to identify deformation mechanisms using only 2D cross-sectional slices as only one cross section of the fibre is visible at a time. Figure 5(c) shows

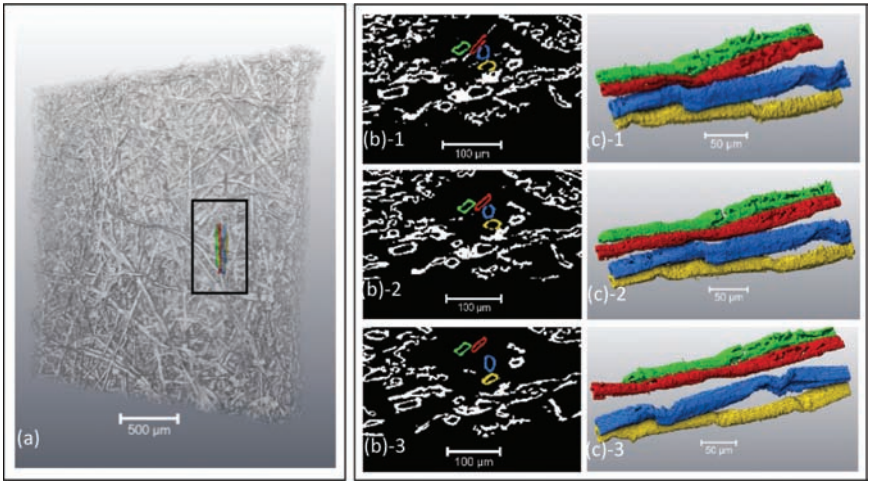

Figure 5. (a) 3D visualization of the freeze-dried sample after being deformation to 1200 µm; (b) Cross section of the same sample and (c) segmented fibres in the region of interest at "-1" reference state, "-2" deformation of 1000 µm, and "-3" deformation of 1200 µm.

a 3D visualization of the four manually segmented fibres from the region of interest: (c)-1 in the reference state, (c)-2 after deformation of 1000 µm, and (c)-3 after deformation of 1200 µm. These fibres have been rotated 90° for ease of display, and thus the loading direction is horizontal. By comparing these figures, it is evident that the process of deformation resulted in a straightening of the red and green fibres, and that this straightening led to an increase in the separation between the red and the blue fibres near the leftmost kink of the blue fibre. Further, although the blue and the red fibres became completely detached from each other, the red and the green fibres remained attached. It also appears that the blue and yellow fibres translated towards the left, suggesting that they were being pulled out. Overall, these observations show that in a freeze-dried handsheet, an increase in fibre separation due to fibre straightening occurs during the early stages of deformation, while complete detachment, i.e. inter-fibre bond breakage, is more prevalent at later stages of deformation, resulting in failure.

3.2 Effect of processing on auxetic behaviour

Paper is known to be an auxetic material, and therefore, due to its negative Poisson's ratio, the thickness will expand under in-plane tension [6], [8]. The extent of the auxetic behaviour in the freeze-dried, non-refined, and highly-refined

samples is explored in Figure 6. In this image, vertical cross-sectional views of all three samples are shown in the (1) reference, and (2) failure states. Further, the failure regions are shown by dashed-line rectangles. First, the freeze-dried sample is seen to have undergone significant thickness expansion during deformation, Figures 6(a)-1 and 6(a)-2. As observed in Figure 5, this occurred because of increased separation between the fibres during deformation followed by complete detachment and pull-out of the fibres. Second, the non-refined sample is also seen to have undergone thickness expansion during deformation, Figures 6(b)-1 and 6(b)-2, in the failure region. However, the amount of expansion is less than what is observed in the freeze-dried case. Third, the highly-refined sample, Figures 6(c)-1 and 6(c)-2, showed relatively little thickness expansion prior to failure. Considering that the non-refined sample is expected to have weaker inter-fibre bonding compared to the highly-refined sample as a result of lower conformability of its constitutive fibres, and the fact that the freeze-dried sample is expected to have weaker inter-fibre bonding compared to the non-refined sample (as freeze-drying is believed to reduce the Campbell effect during drying), the auxetic behaviour seems to be strongly correlated to the extent of the inter-fibre bonding in the sample. From these observations, it is clear that the auxetic behaviour is minimized when the extent of the inter-fibre bonding within a handsheet is increased.

3.3 Measured loads during deformation

Figure 7 shows the peak loads of all the three tests plotted against the displacements read from the tensile tester. Recall that each test contained multiple samples, four for the non-refined and highly-refined tests and three for the freeze-dried test. As can be seen, the load peaks at 32 (N) for the highly-refined test at a displacement of 1400 μm, then drops sharply afterwards, while for the non-refined and freeze-dried tests the values are 19 N and 8.5 N at displacements of 1200 μm and 1000 μm. The significant drop in the load after the peak value is associated with the failure of one or two samples within a test. Interestingly, for the highly-refined and non-refined samples, there is a slight increase in the load a few steps after the peak, after which it drops again to zero. This behaviour is associated with the deformation and failure of the remaining samples that had not previously failed. This post-peak increase is not seen for the freeze-dried test, as the failure of all the samples for this sample happened almost simultaneously. Further, the load drop for the freeze-dried sample is not sudden and it drops rather smoothly. This is because the freeze-dried samples are thought to have low contribution from fibre fracture as a result of their very weak inter-fibre bonding, and consequently, the fibres were physically in contact even after failure until they were completely pulled out.

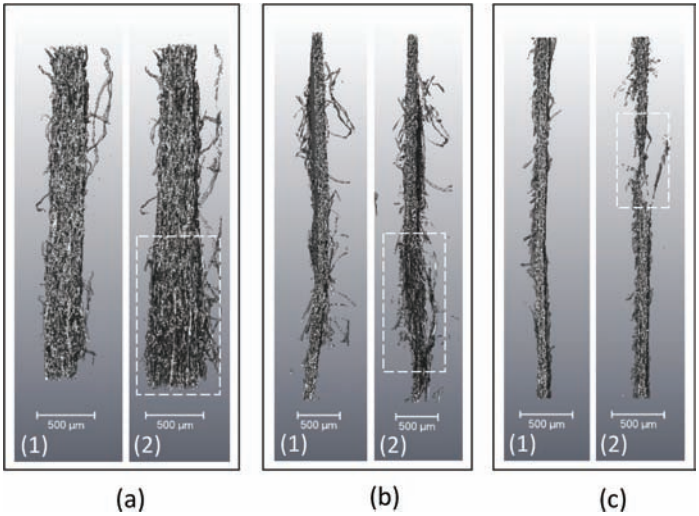

Figure 6. Vertical cross section views of the (a) freeze-dried, (b) non-refined, and (c) highly-refined samples in the reference state (1) and after failure (2). The dashed-line rectangles show failure regions.

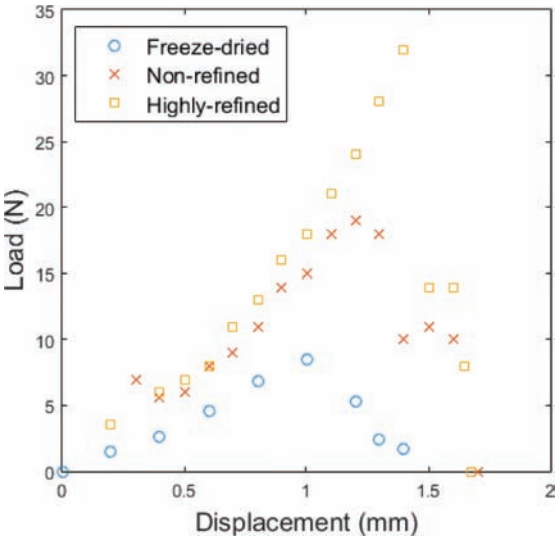

Figure 7. Peak load of the freeze-dried, non-refined, and highly-refined 4D imaging tests as a function of P2R tensile-tester cross-head displacement

3.4 Quantitative Insights

Figure 8 shows strain contours from the DVC analysis, along with the corresponding 3D visualizations of the failed states of the freeze-dried (*left*), non-refined (*middle*), and highly-refined (*right*) samples. The 3D visualizations are given in the top row. As can be seen, definitive rupture zones were captured for both the non-refined and highly-refined samples. From these images, one can see that the number of un-broken fibres in the rupture zone is greater in the non-refined sample as compared to the highly-refined sample. Further, there is an even larger number of un-broken fibres in the bottom part of the freeze-dried sample. This provides strong indication that an increase in the extent of inter-fibre bonding in the samples significantly reduced the role of fibre pull-out in handsheet deformation and failure.

The middle row of Figure 8 shows the DVC calculated out-of-plane (ε_{yy}) strain fields measured from the acquired sCT datasets for each of the three samples at the point just prior to failure. The yellow regions identify a strain value greater than 0.24, while the red regions identify areas of low strain. A comparison between these strain fields reveals that the extent of yellow regions increases right to left, i.e. the extent of inter-fibre bonding decreases. This is consistent with the observations from Figure 6 in terms of thickness expansion in the freeze-dried, non-refined, and highly-refined samples.

The bottom row of Figure 8 shows the corresponding in-plane (ε_{zz}) strain fields; the yellow and red regions identify areas with high and low in-plane deformation. As can be seen, there is a large region of high in-plane deformation at the bottom of the freeze-dried sample that is consistent with the previous observations that showed the fibres were being pulled-out from the bottom of the freeze-dried sample. Further, a comparison between the in-plane and out-of-plane strain fields of this sample shows that large out-of-plane deformations seem to be concentrated in areas associated with high in-plane deformations. From the non-refined sample, it is evident that there is also a narrow band of large in-plane deformation occurring near the top. For the most part, the large out-of-plane deformations in this sample occur in regions neighboring the large in-plane deformations. The highly-refined sample contains very few regions that show large deformations, both in-plane and out-of-plane.

The results shown in Figure 8 quantify the observations from Figure 6, that is, the freeze-dried and non-refined samples show significant auxetic behaviour while the highly-refined sample only shows minimal auxetic behaviour. Although the regions of large in-plane deformation for the freeze-dried and non-refined samples clearly correspond to the failure regions seen in the 3D images, the same cannot be concluded for the highly-refined sample. Perhaps, in this sample, the region that later resulted in rupture was not captured in the initial 3D image, and

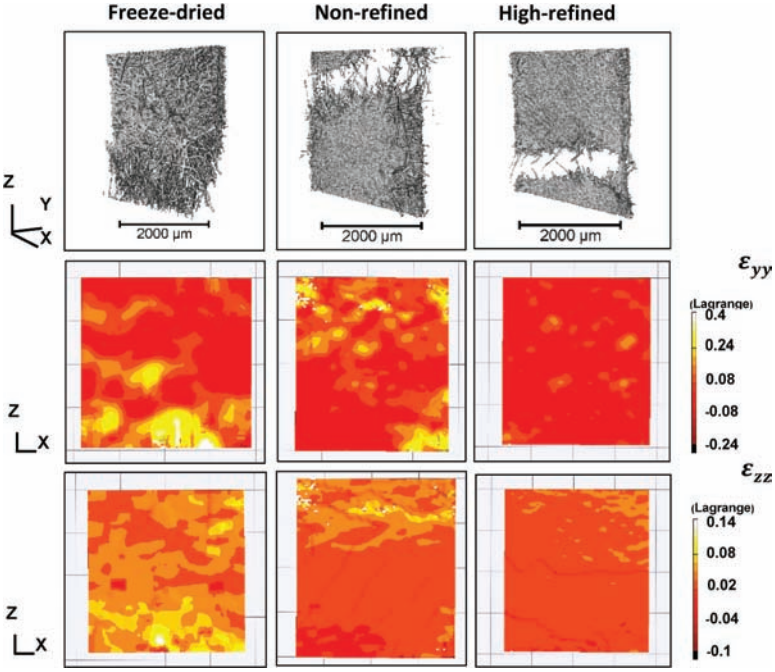

Figure 8. 3D image of the failed state of the freeze-dried (*left*), non-refined (*middle*) and highly-refined (*right*) samples along with the DVC calculated strain fields in the out-of-plane and in-plane directions.

therefore, excluded during the DVC calculations. Alternatively, the high-refining led to brittle fracture that was not captured by the 4D imaging process. However, this does not undervalue the observations of the out-of-plane deformations, since any large out-of-plane deformations resulting from increased fibre separation and detachment, would still have been visible in the DVC-calculated strain fields.

Figure 9 plots the L2 norm of the out-of-plane strain fields, N_{yy} against the P2R cross-head displacement for all the three samples. The arrows indicate the displacement stage that correspond to the first or second load peak in the load-displacement curve of each sample in Figure 7. Note that the results shown in Figure 9 correspond to samples that failed just after the second load peak was reached. As can be seen, all three samples show the same trend, an increase in N_{yy} occurs with an increase in displacement, which is consistent with the

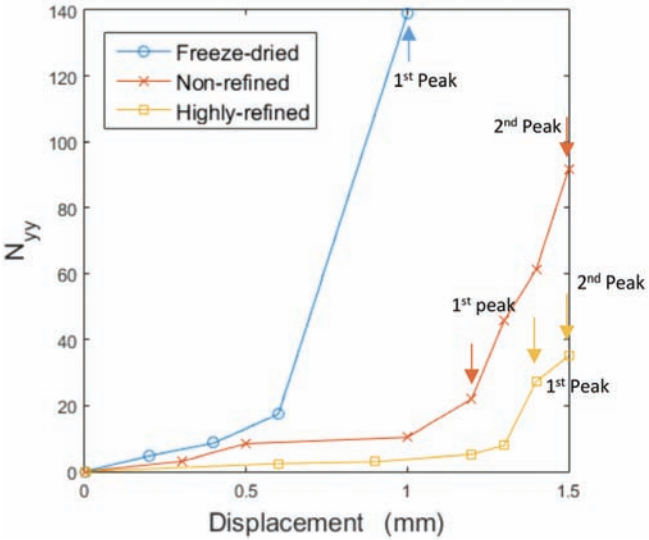

Figure 9. The norm of the out-of-plane strain field, N_{yy} from the DVC analysis as a function of the P2R cross-head displacement for all three samples

expected auxetic behaviour of paper. However, while there is a relatively large increase in N_{yy} at later stages of deformation, the increase is small early-on. Thus, for all samples, a best-fit line to this data would be second-order, which is consistent with the literature [5], [7], [8]. This is also consistent with the observations in Figure 5 where only a small increase in the separation of fibres was observed at the early stages of deformation, while complete fibre detachment was only seen just prior to failure. In general, the values for N_{yy} increase when the extent of inter-fibre bonding decreases. Interestingly, the difference amongst the values of N_{yy} for different samples increased drastically at the later stages of deformation where fibre detachments were observed. This suggests that inter-fibre bond breakage is the main factor responsible for the difference in the accumulated out-of-plane deformations of the three samples. Considering that inter-fibre bond breakage is a precursor to fiber pull-out, we propose that the accumulated out-of-plane deformations can be used to quantify the contribution of fibre pull-out towards failure in paper handsheets. One should also note that the lines plotted between the measurement points do not imply a linear change between them, but instead were added to facilitate the comparison between the three samples.

4 SUMMARY

In this study, 4D imaging using synchrotron X-ray computed tomography has been applied to investigate the deformation mechanisms of NBSK paper handsheets. It was shown that the acquired 3D data can be used to evaluate the deformation mechanisms active within freeze-dried, non-refined, and highly-refined samples. Qualitative observations at the network level revealed the auxetic behaviour of samples, which was shown to be related to the paper making process parameters through the degree of inter-fibre bonding. Observations at the fibre level revealed different deformation mechanisms being responsible for the auxetic behaviour: fibre separation due to fibres being straightened at the earlier stages of deformation along with complete fibre detachment during the later stages of deformation.

Using DVC, the local out-of-plane and in-plane deformations were quantified; the inter-fibre bond breakage was shown to be the main contributing factor to the observed differences between samples in terms of the amount of out-of-plane deformation. Therefore, via sCT, the out-of-plane strain fields during in-plane tension can be used to quantify the fraction of inter-fibre bond breakage during tensile deformation of paper handsheets. Considering that inter-fibre bond breakage is a precursor to fibre pull-out, this method could be used in the future to quantify the relative contribution from fibre pull-out and fibre breakage to handsheet failure.

ACKNOWLEDGEMENTS

The authors thank Canfor Pulp Inc., the Natural Sciences and Engineering Research Council of Canada (NSERC) and MITACS for funding this work. Further, this work was made possible by the facilities and support provided by the Research Complex at Harwell, funded in part by the EPSRC (EP/I02249X/1 & EP/M009688/1). Further, we thank the Diamond Light Source for providing the beam-time (MT13240) and staff at I13 beamline for technical support.

REFERENCES

1. H. F. Rance, “The formulation of methods and objectives appropriate to the rheological study of paper,” *Tappi J.*, **2**:104–115, 1956.
2. M. Perez, “Model for Stress-Strain Properties of Paper,” *Tappi J.*, **53**(12): 2237, 1970.
3. K. I. Ebeling, “Distribution of Energy Consumption during Straining of Paper,” Lawrence University, Appleton, Wisconsin, 1970.

4. J. Kubát, "Rheology of Paper," in *Rheology, Volume 5*, F. R.. Eirich (ed.), New York: Academic Press, 1969, pp. 547–602.
5. O. Öhrn, "Thickness variation of paper on stretching," *Sven. Papperstidning*, 1965.
6. N. Stenberg and C. Fellers, "Out-of-plane Poisson's ratios of paper and paperboard," *Nord. PULP Pap. Res. J.*, **17**(4):387–394, 2002.
7. P. P. Post, C. Berger, K. Villforth, H.J. Schaffrath and S. Schabel, "Optical measurement of deformation of paper under tensile load," *Nord. Pulp Pap. Res. J.*, **27**(2)313–317, 2012.
8. P. Verma, M. L. Shofner and A. C. Griffin, "Deconstructing the auxetic behavior of paper," *Phys. Status Solidi Basic Res.*, **251**(2):289–296, 2014.
9. W. B. Campbell, "The cellulose-water relationship in paper-making," in *Forest Service Bulletin 84*, Ottawa, 1993.
10. R. H. Marchessault, "The effect of freeze-drying on the physical properties of cellulose fibres and papers," McGill University, 1954.
11. J. V. Robinson, "Fibre Bonding," in *Pulp and Paper:Chemistry and Chemical Technology, Vol II* (3rd edn), J. P. Casey (ed.), New York: John Wiley & Sons, 1960, pp. 915–963.
12. C. Puncreobutr, P. D. Lee, R. W. Hamilton and A. B. Phillion, "Quantitative 3D characterization of solidification structure and defect evolution in Al alloys," *Jom*, **64**(1):89–95, 2012.
13. B. K. Bay, T. S. Smith, D. P. Fyhrie and M. Saad, "Digital volume correlation: Three-dimensional strain mapping using X-ray tomography," *Exp. Mech.*, 39(3): 217–226, 1999.
14. B. K. Bay, "Methods and applications of digital volume correlation," *The Journal of Strain Analysis for Engineering Design,*. 2008.

Transcription of Discussion

SYNCHROTRON TOMOGRAPHIC IMAGING OF SOFTWOOD PAPER: A 4D INVESTIGATION OF DEFORMATION AND FAILURE MECHANISM

F. Golkhosh,[1] *Y. Sharma,*[2] *D. M. Martinez,*[3] *W. Tsai,*[3, 4] *L. Courtois,*[5] *D. Eastwood,*[5] *P. D. Lee*[5] *and A. B. Phillion*[6]

[1] School of Engineering, The University of British Columbia, Canada
[2] Chair of Biomedical Physics, Department of Physics and School of BioEngineering, Technical University of Munich, Germany
[3] Dept. of Chemical and Biological Engineering, The University of British Columbia, Canada
[4] Canfor Pulp Innovation, Canfor Pulp, Canada
[5] Manchester X-ray Imaging Facility, University of Manchester, UK
[6] Dept of Materials Science and Engineering, McMaster University, Canada

Artem Kulachenko KTH Royal Institute of Technology

I have two questions. First, what was the solid content before you started the freeze drying?

André Phillion McMaster University, Canada

This was not measured. But, it was a standard handsheet.

Artem Kulachenko

Also, in one of the slides you showed the video where you visualized the in-plane strain, and you could see immediately right from the start that the strain localizes and you have a fracture, but in the previous slide you showed a sequence in which

the localization at fracture happens at a place different to where you have strain concentrations initially.

André Phillion

Yes, you are absolutely right. These images were made for the article that we wrote and then last week I asked the graduate student working with us to make this video, so it would appear that this video is reversed 90 degrees as compared to the other one.

Artem Kulachenko

Do you have a possibility to see if there is a gradient of the in-plane strains in the thickness direction because currently you average the strain over the thickness?

André Phillion

Yes. So you have the entire volumetric strain field and this is what is shown on the surface. But you have the entire thickness data, so at every point in the volume, the software will tell you what the strain field is at that location.

Jonathan Phipps FiberLean

You explained that when you setup the samples, there were 4 strips in a row, and there were some small spacers between them which were then glued to the samples. What influence did they have on the deformation mechanism itself and did they break before the paper sample or simultaneously with it?

André Phillion

That is a good question. In order to create these samples we had to put holes in the sheet so we could affix them to the grips, and so we put a very small amount of adhesive in the clamp area to reinforce the grip. All of the samples shown here failed in the gauge length and not in the grip. If they failed in the grip, then we discarded that data.

Jean-Francis Bloch Grenoble Institute of Technology

I do have problems with your presentation and the first one is, I have been taught that when I want to tackle a problem, I have to define it, look at the literature which some people have done on the same topic. You may criticise the articles

and, then you may try to improve the knowledge. Here, I don't find any reference about the work in literature. Not a word about what has been done in Finland or in France. So afterwards it's very easy to write 'for the first time', and its completely wrong. DIC, for example has already been coupled with tomography, it has been published, as well as time dependence, and therefore I think in particular in this conference, with all the respect I have for this conference, it is not acceptable at all. That is my first point. Then, I will go into more details about your presentation. Did you check that, for example, you have any effect of the x-ray on the rheological behaviour you have shown here?

André Phillion

Yes, we checked them and there is some effect, there was some discoloration of the paper that occurred during tests.

Jean-Francis Bloch

I don't speak only on the discoloration which is well known. But it has been shown that you have to control *in situ* humidity. You should test exactly the same situation with and without x-ray, to prove that you have no effect from the X-rays, on the mechanical behaviour. That is the way we have been running experiments for almost 20 years: we maintain (or not) a constant humidity. If you don't know the initial moisture content, or the humidity, you will have a lot of variation that makes it difficult to analyse. Finally, we know that the mechanical behaviour is viscoelastic. Therefore it is completely different to make what we call an 'interrupted test': where you stop the test to take a 3-D image, after which you start it again. What was shown is that you can do that in a continuous way, the behaviour is different. So what was your way of carrying out the experiment exactly? Did you make some interrupted tests or carry out these in a continuous way?

André Phillion

We measured the load continually, however, the deformation was interrupted. Between the deformation steps, there were some small changes in the measured loads. As for your other comments, I agree with you that DIC has been performed previously, I haven't stated that this is the first time that DIC has been applied to paper, but here we focused on DVC, and 3-D imaging, not 2-D techniques. During these experiments, we made a great effort to ensure that the conditions remained constant (e.g. humidity) and were performed in a controlled manner. In doing so, we were able to acquire some very nice visualizations of deformation mechanisms under different refining conditions.

Discussion

Jean-Francis Bloch

I just may encourage you to read for example, the papers from Pierre Dumont who did the same thing for bending, or for fracture. I am sure you will find it interesting and you will save a lot of time introducing into your research what has been done recently.

Tetsu Uesaka Mid-Sweden University

I am just wondering what is the motivation for using this sample size?

André Phillion

We chose that sample size because we wanted the sample to fit in the entire cross-section that was available in the X-ray field of view. If we had used a larger sample size, then we wouldn't have had the entire cross-section in the field of view, or the image resolution would have been lower. The chosen resolution and sample size were a compromise to achieve good experimental results.

Tetsu Uesaka

So, do you need to correct for the sample size?

André Phillion

I would agree with you that you would need to correct for sample size if we were talking about the applied loads, if we had reported the failure stress or failure strain in the material. But, in terms of understanding what the micromechanics are, the sample size is so much larger than the width of the fibres so that the results remain relevant.

Warren Batchelor Monash University

Would you be able to track individual fibres, so that you could look at really getting down to what is happening in the fibres and bonding, and the micromechanics in detail.

André Phillion

At this level of resolution, we can image individual fibres, but we can't really image or quantify anything about the contact area between the fibres or the degree of delamination that occurs with increasing deformation.

Vikram Singh Raghuwanshi Monash University

What X-ray energy did you use?

André Phillion

We used the pink beam, which is a range of energies where the very low energy X-rays are filtered out to improve signal to noise ratio. The X-ray energy range was 5–20 KeV. One cannot use a monochromatic beam because a high flux is needed to acquire the 3-D image in a reasonable amount of time.

Vikram Singh Raghuwanshi

What was the detector distance from the samples?

André Phillion

I don't recall that. It was sufficiently close to avoid phase contrast effects.

Vikram Singh Raghuwanshi

My final question is that when you measure it, how do you rotate the sample? You rotate and then how long do you measure it for?

André Phillion

We acquired 1,800 radiographs, each at 100 ms.

Jean-Francis Bloch Grenoble Institute of Technology

Your question is excellent because usually you can have different distances between the sample and the detector. It may be modified when you want to obtain some phase contrast. So, depending on the kind of sample you have, you may modify this distance. What you need to know is that it is a technical technique, called holotomography, where you take 3-D images at different distances. You obtain a much better quality, but you are restricted to static studies. You can also have, if needed, with the same samples what we call multi-resolution imaging. That is to say you can have for a given sample, different 3-D images at different resolutions. You choose a small zone and then you can have a much better focal resolution depending on what you want to see. These techniques were published.

Discussion

André Phillion (added afterwards)

All of what J.-F. Bloch says is true, but the focus in this work was on imaging deformation. The experimental procedures were chosen to minimize viscoelastic effects and beam damage, have not achieved the highest resolution possible.

Doug Coffin Miami University, Oxford, OH

Of the four fibres we chose here, were they bundled together, because they are all aligned very well and straight. Can you go back and pick four fibres like that that cross each other, so that you should be able to pick out multiple places and track fibre network deformation.

André Phillion

In theory, you can identify and track any fibre. We developed a tracking algorithm for fibres that have open lumens like these four shown here. But if the fibres are collapsed, then it requires manual tracking and segmentation.

Doug Coffin

I would also be interested in seeing the deformation of a small network of fibres and how that deforms over time in the tests.